POLITECNICO DI TORINO
Repository ISTITUZIONALE

Skyrmion velocities in FIB irradiated W/CoFeB/MgO thin films

(Article begins on next page)

03 May 2024

Skyrmion velocities in FIB irradiated W/CoFeB/MgO thin films ⓔⓟ

Valentin Ahrens, ⓘⒹ Luca Gnoli, Domenico Giuliano, et al.

COLLECTIONS

View Online   Export Citation   CrossMark

Call For Papers!

AIP Advances

SPECIAL TOPIC: Advances in
Low Dimensional and 2D Materials

Skyrmion velocities in FIB irradiated W/CoFeB/MgO thin films 🔵EP

View Online   Export Citation   CrossMark

Valentin Ahrens,[1,a)] Luca Gnoli,[2] 🆔 Domenico Giuliano,[2] Simon Mendisch,[1] 🆔 Martina Kiechle,[1] 🆔
Fabrizio Riente,[2] 🆔 and Markus Becherer[1,b)] 🆔

AFFILIATIONS

[1] Nanomagnetic Devices Group, Chair of Nano and Quantum Sensors, Department of Electrical and Computer Engineering,
 Technical University of Munich, Munich, Germany

[2] Department of Electronics and Telecommunications, Politecnico di Torino, Torino, Italy

Note: This paper was presented at the 15th Joint MMM-Intermag Conference.
[a)] Author to whom correspondence should be addressed: valentin.ahrens@tum.de
[b)] Electronic mail: markus.becherer@tum.de

ABSTRACT

In recent years magnetic skyrmions attracted great attention for the possibility to move them with low current density, their intrinsic stability and their robustness against defects and edge roughness compared to other magnetic textures. For applications, it is very important to be able to influence the behaviour of skyrmions locally. In this article, we present an evaluation on the effects of FIB Ga^+ irradiation on skyrmion motion in W/CoFeB/MgO thin films. The influence of FIB irradiation is evaluated both, in terms of modification of the skyrmion Hall angle and the skyrmion velocity. An overview of the effects of the pulsing parameters on the skyrmion motion, shows low influence of the pulses rise-time and an external magnetic field. In addition the analysis after the irradiation shows that it influences notably the dynamics of skyrmions. In the irradiated zone the speed and angle of motion of these magnetic textures are strongly reduced.

I. INTRODUCTION

Skyrmions, topologically protected spin-textures, were first discovered in the early 2000s,[1] after their theoretical prediction in the late 1950s.[2] From that point on, their possible use in racetrack memories,[3–5] oscillators[6] and logic gates[7,8] has been proposed and examined in numerous works. Simulations demonstrated how spintronic memories and logic based on skyrmions are comparable or superior to the CMOS counterpart regarding area, latency, and energy consumption for special applications.[9,10] Some of the most intriguing properties of skyrmions are the possibility to move them with low current densities, their intrinsic stability due to topological protection, and predicted robustness against defects and edge roughness with respect to other magnetic textures.

Skyrmions are nowadays easily stabilized by out-of-plane magnetic fields in the few mT regime.[11–13] Motion is commonly driven by charge currents utilizing spin-orbit-torques.[14–16]

One key issue on the way to realize skyrmion devices is the ability to control and synchronize their motion. Shift registers based on voltage-controlled magnetic anisotropy[17] or potential wells in an anti-dot lattice[18] are envisioned candidates for his purpose. Furthermore, it is essential to control the skyrmion Hall effect, which leads to a partial deflection of the skyrmions in the transverse direction with respect to the current direction.[13,16] It has been shown that skyrmions can be nucleated at focused ion beam (FIB) irradiated spots.[19,20] Furthermore local He^+ irradaition has been used to create skyrmion tracks[14] and FIB Ga^+ irradiation to confine skyrmions.[21]

To assess how areal Ga^+ ion irradiation can be used to engineer the trajectories of skyrmions, we evaluated skyrmion motion, driven by currents, in focused ion beam treated magnetic wires.

As a basis for our experiments, we produced trilayers of the frequently used W/CoFeB/MgO system that has been shown to host skyrmions.[15] The same material combination is used as a free

layer in the SOT-MRAM technology,[22] which makes it promising for skyrmion technology. We show that we can achieve a stable skyrmion phase in these films by post-deposition annealing in a N_2 atmosphere. Skyrmion films are patterned into wires and contacted electrically. Moving a large amount of skyrmions with current pulses, we can evaluate with good statistics the current-driven motion of skyrmions. We analyze the data for current-driven motion of skyrmions in pristine and irradiated films and explore the possibilities to tailor their trajectories.

With this work, we provide a powerful strategy for FIB irradiation as a versatile means to engineer the velocity and angle of current-driven skyrmions in sputtered thin-films. The proposed technique in contrast to other works[14,21] uses areal low dose irradiation.

II. METHODS

Trilayers consisting of W (3)/$Co_{20}Fe_{60}B_{20}$(0.9)/MgO(1)/Ta(1), with the thicknesses of the individual layers given in nm, are sputtered using a home-built RF magnetron sputtering tool (base pressure $\approx 1 \times 10^7$ mbar). Annealing at 275 °C in a N_2 atmosphere is used to adjust the magnetic properties. We confirm the formation of a stable skyrmion phase at low magnetic fields by polar widefield magneto-optical Kerr-effect (WMOKE) microscopy. For hysteresis measurements, focused laser MOKE (LMOKE) measurements

are utilized. After annealing, the samples are capped with a 3 nm thick sputtered tantalum layer to protect the film during the following processing steps. Suitable films (with a skyrmion phase) are structured into 25 μm and 35 μm wide magnetic wires by optical lithography and ion beam etching. These wires are then contacted electrically using optical lithography and physical vapor deposition of a Cu/Cr layer. One half (12.5 μm and 17.5 μm respectively) of the contacted magnetic wires is irradiated with a scanning 50 keV Ga^+ focused ion beam as indicated in Fig. 1d) and e). The ion beam has a nominal width of 5 nm however we expect the actual affected area to be around 10 nm to 20 nm due to unideal focusing and scattering of the ions in the thin film. The used doses ranges from 1×10^{12} ions/cm^2 to 5×10^{12} ions/cm^2.

In Fig. 1a) the printed circuit board as chip-carrier is depicted, hosting a (b) wire-bonded chip in order to excite skyrmions with current pulses. The pulses have a width ranging from 25 ns to 400 ns and a rise-time of 1.8 ns. The current density was varied from 0.8×10^{11} Am^{-2} to 2×10^{11} Am^{-2}, details about the measurement of the pulse current are given in the supplementary material. To measure the skyrmion velocity, first, a domain image is taken, second a current pulse is applied to the wire and third the domain structure is imaged again and differences are recorded as shown in Fig. 1d-e). Repeating this procedure several times videos of the moving skyrmions (snapshot after each pulse) can be created (see Fig. 1 (Multimedia view)). From the differences between two consecutive
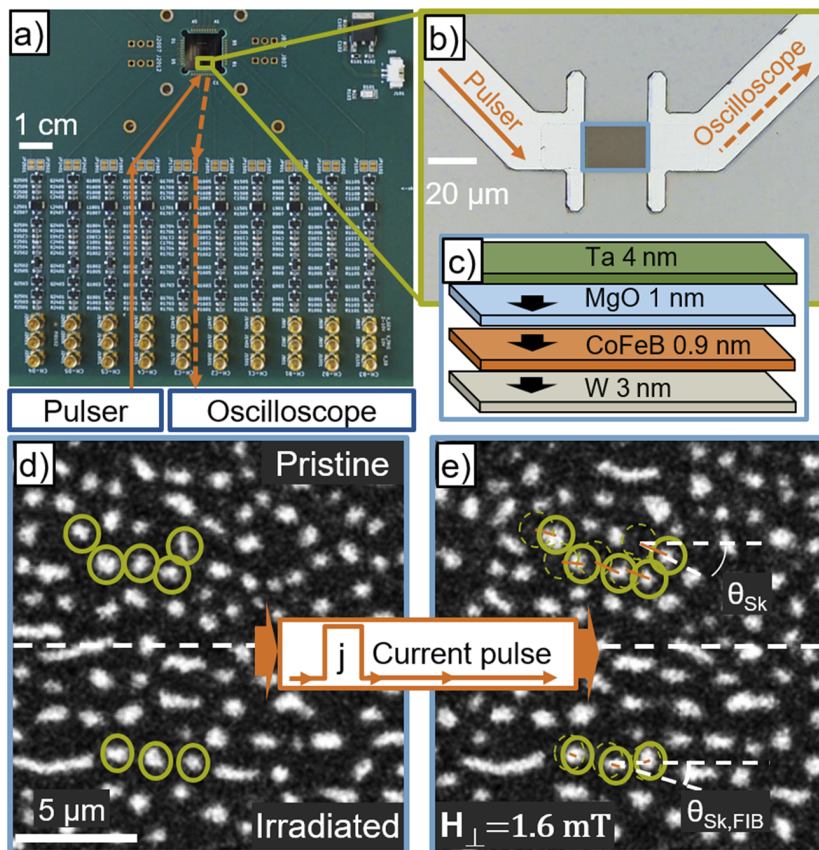

FIG. 1. Overview of the measurement setup. a) Image of the used chipcarrier with the current path indicated from the pulser along a direct coaxial connection (without components) to the sample and after passing the wire back via a second channel to the oscilloscope. b) Microscope image of a magnetic wire with the on chip connectors on the left and the right. c) Visualization of the thin film stack, the skyrmion hosting magnetic wires are made of. d) and e) WMOKE images of the wire before (d) and after (e) a burst of four current pulses with a width of 50 ns and a rise-time of 1.8 ns and a current density of $\approx 1.75 \times 10^{11}$ Am^{-2} measured at a constant field of 1.6 mT. The same skyrmion ensemble (green circles) is marked in d) and e) for the upper pristine part and the lower part that was irradiated with a dose of 1.12×10^{12} ions/cm^2. In the image e), taken after the pulse, also the previous location of the skyrmion ensemble is marked with dashed green circles and their trajectories in orange. Furthermore the sykrmion Hall angle is indicated in e) for the pristine part (P) (θ_{Sk}) and the irradiated part (I) ($\theta_{Sk,FIB}$). A skyrmion motion video of the same wire with overlayed tracks is given in the (Multimedia view). Multimedia view: https://doi.org/10.1063/9.0000287.1

frames the displacement of the individual skyrmions due to the current pulses can be extracted as illustrated in the images. Dividing the displacement by the pulse time we gain the skyrmion velocity. Geometrical considerations give the skyrmion Hall angle i.e., the deviation of the skyrmion motion from the current direction. The motion of at least 100 skyrmions is tracked for each video and averaged to gain a statistically sound estimate of the skyrmion velocity and the skyrmion Hall angle. We used the TrackMate algorithm of Fiji,[23,24] to track such large amounts of skyrmions. TrackMate is able to detect the location of spots (skyrmions) and track their motion based on the mathematical framework of a linear assignment problem. The tracking parameters, i.e., the radius estimate (r_{est}) for spot detection and maximum linking distance (d_{max}) for tracking, were fixed for all measurements to r_{est} = 600 nm and d_{max} = 1500 nm. Manual inspection has verified the track results for this settings to be at least 95 % correct.

Further analysis has shown that changes of the tracker parameters in the range of ±30 % only result in changes <10 % in the measurement results.

III. RESULTS AND DISCUSSION
A. Post-deposition annealing

As noted above, the thin films are annealed in a rapid-thermal-processing (RTP) tool in a N_2 atmosphere. A first 5 min annealing step is needed to achieve an out-of-plane magnetization in the samples. From that point on, each annealing step reduces the coercive field, as illustrated in Fig. 2.

This degradation is likely associated to a reduction of the effective anisotropy. One reason for that can be a reduction of the interfacial anisotropy due to thermal degradation of the CoFeB – MgO interface, which is the main contribution to the PMA in metal/ferromagnet/oxide layers.[25] As well an increase of the saturation magnetization M_s is proposed[26] as also a reduction due to diffusion of Fe into the W layer and a growth of the magnetic

FIG. 2. LMOKE hysteresis loops after 5 min (blue), 10 min (orange) and 25 min (green) of annealing. The images show the domain state at different magnetic fields as indicated by the arrows after annealing for 25 min.

dead layer.[27] At a specific annealing time, in our case 25 min, we observe a reduction of the coercive field to 0 mT and an hourglass-shaped hysteresis as often presented for skyrmion films.[28,29] We imaged the static domain structure, at this annealing step, at different fields. From these measurements, we can confirm the coexistence of skyrmions and domains as shown in the images in Fig. 2, with its majority shifting from domains to individual skyrmions from 0 mT to 2.5 mT.

B. Skyrmion motion

While having claimed the existence of a stable skyrmion phase in the previous section, up to now we only have shown that we can stabilize circular shaped domains. To prove that these domains are actually skyrmions, i.e., that their topological charge Q is equal to 1, we assess their current-driven motion. This motion is commonly described by a modified Thiele equation[13]

$$\boldsymbol{G} \times \boldsymbol{v}_{Sk} + \alpha \boldsymbol{D} \boldsymbol{v}_{Sk} + 4\pi B \boldsymbol{j} = 0. \tag{1}$$

Where G = $(0, 0, -4\pi Q)$ is the gyromagnetic coupling vector that attributes for the Magnus force on the skyrmion. The skyrmion drift velocity is denoted v_{Sk}, α is the magnetic damping and D the dissipative tensor that combines all dissipative contributions to the skyrmion motion. Finally, B is the efficiency of converting the electrical current j in the W layer into driving force for the skyrmion, via the spin Hall effect. From this equation we can derive the ratio of skyrmion velocity in x and y direction ($v_{Sk,x/y}$) as $\frac{v_{Sk,x}}{v_{Sk,y}} = \frac{-Q}{\alpha D}$. The skyrmions move under an angle to the current direction while topologically trivial structures (Q = 0) move straight or expand. Moreover, in our experiments, the angle of motion is mirrored along the current direction for changing Q from +1 to −1. Practically this change, reversing the magnetization of the background and the skyrmion core, is achieved by inverting the sign of the external magnetic field. To limit Joule heating it is essential to keep the current pulse time in the sub μs regime. For more detailed information about the current pulse measurements the reader is referred to the supplementary material.

1. Pulse dependence

To out-rule effects of the pulse-shape on the skyrmion velocity we swept the rise-time of the pulse (t_{rise}) from 1.8 ns to 200 ns while keeping the pulse current at ≈ 1.36×10^{11} Am^{-2}, the pulse-width at 200 ns and the external field ($\mu_0 H_{ext}$) at 1.6 mT. For rise-times up to 50 ns no change in the skyrmion velocity v_{Sk} can be measured. Above that, the velocity slightly drops as shown in Fig. 3a). This can be explained by a critical current density j_{crit} that is needed to move a skyrmion in a given track. For higher t_{rise}, the effective time the pulse surpasses j_{crit} is reduced. The skyrmion Hall angle θ_{Sk} remains utterly unaffected by changes of t_{rise}.

Accordingly to the rise-time the effects of the pulse-width (t_{pulse}) from 20 ns to 400 ns were analyzed fixing the summed up pulse time to 400 ns by applying bursts of pulses with μs separation and the respective pulse number to reach 400 ns. Again, the current density was set to 1.36×10^{11} Am^{-2}, t_{rise} to 1.8 ns and the external magnetic field to 1.6 mT. Here, in Fig. 3b), for low pulse-width < 50 ns a decrease of the skyrmion velocity is apparent.
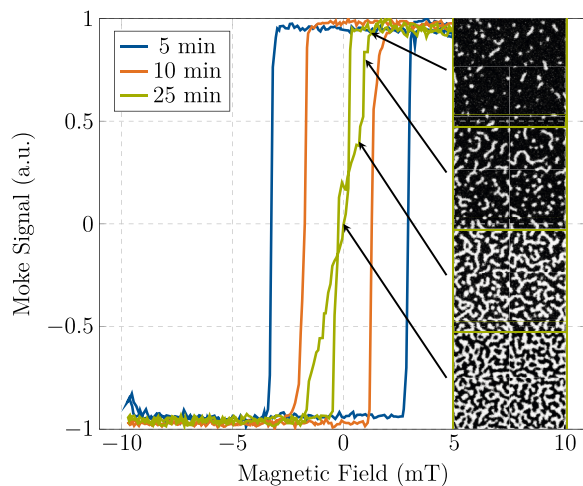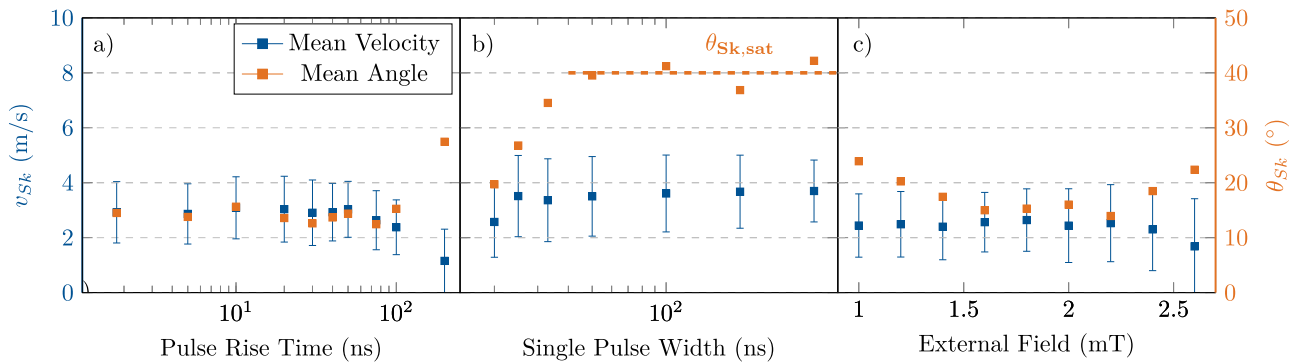
FIG. 3. Overview of the effects of Pulse rise time t_{rise} (a) Pulse width t_{pulse} (b) and external magnetic field $\mu_0 H_{ext}$ (c) on the skyrmion velocity v_{Sk} (blue squares) and Hall angle θ_{Sk} (orange squares). Apart from the varied parameter, all parameters were set to $j_{pulse} \approx 1.37 \times 10^{11}$ Am^{-2}, $t_{pulse} = 50$ ns, $t_{rise} = 1.8$ ns, $\mu_0 H_{ext} = 1.6$ mT. In b) the saturation skyrmion Hall angle $\theta_{Sk,\,sat}$ is indicated by the dashed orange line.

One possible explanation is that for short pulses also the effective pulse time is diminished due to inductive effects in the conductors that lead to an effectively increased rise-time of the pulses. This alone, however, can not explain the change in skyrmion Hall angle. With increasing t_{pulse} the θ_{Sk} drastically increases at first and then saturates to its intrinsic value of around 40° near to what was shown in other publications.[13] This development can be attributed to a change from depinning dominated creep motion to free flow motion as predicted for systems with quenched disorder by Reichhardt and Reichhardt.[30] Therefore we propose a similar mechanism as for the thermally assisted overcoming of a energy barrier, described by the Néel-Brown model.[31–33] As the depinning is a stochastic thermal effect, short pulses are not always able to depin the skyrmions from their starting point, usually a defect forming a potential well. However as a skyrmion is depinned it can to a certain extent be repelled from defects[34] resulting in a higher v_{Sk} and θ_{Sk} as the motion gets more flow-like. Also the repinning of a skyrmion takes a certain amount of time during that the skyrmion is supposed to spiral towards its the lowest energy state in the pinning site. In turn that means that while moving, the depinning energies for the skyrmion are lower, and therefore easily overcome by the applied current. Beyond that, longer pulses will aggravate the effect of joule heating that further contributes to a less pinning dominated motion and a larger θ_{Sk}.

2. Field dependence

It is essential to exclude the effects of skyrmion-skyrmion interaction on the skyrmion velocity and the skyrmion Hall angle, to perform a statistical evaluation with many skyrmions. As shown in Fig. 2 we can use the external field to adjust the skyrmion density in a broad range. Therefore one appealing option to rule out such interactions is to analyze skyrmion motion with changing external magnetic field. We found that skyrmions can be stabilized and moved from 1 mT to 2.6 mT. We kept the current density, pulse-width and rise time unvaried at 1.36×10^{11} Am^{-2}, 50 ns and 1.8 ns respectively, and evaluated the motion of skyrmions with changing external field. This reveals that in the field range relevant for this work (1.4 mT to 2.3 mT) no significant effects neither on v_{Sk} nor

on θ_{Sk} are evident, as shown in Fig. 3c). With this data in mind, an effect of skyrmion-skyrmion interaction on their motion in the investigated range seems unlikely. If the magnetic field is increased above 2.2 mT a slight decrease of v_{Sk} can be observed along with an increase of θ_{Sk}. A similar trend on θ_{Sk} is visible for magnetic fields below 1.4 mT. While we do not have a conclusive explanation for this behaviour we here make a phenomenological hypothesis based on our observations. At fields above 2.2 mT only few skyrmions remain stable most likely at strong pinning sites, so their motion might be strongly distracted, whereas for low fields an increased number of domains can disturb the motion of the skyrmions. For us this interesting trends are worth mentioning, though we are lacking a detailed analysis which is out of the scope of this work.

To further give our statistical evaluation a solid basis, we evaluated disturbances of the tracker.[23] For example, TrackMate cannot perfectly distinguish between domains and skyrmions, especially if the domains are ellipsoids in the size range of the skyrmions. At points, the motion of domains is included in the average velocity as well. For a few representative measurements, we made sure, by manual evaluation, that the velocity of domains, as expected, is on average much lower than that of the skyrmions. While resulting in the worst case in reducing the average velocity, manual exclusion of the domain motion tracks did not result in a relevant change of the average velocities.

The evaluation of far over 100 skyrmion tracks for each data point (except the ones for a very high or very low external field, due to a low number of skyrmions) nearly inevitably leads to a particular normally distributed spread of values for individual tracks. In turn, this leads to the high standard deviations the reader can see in the plots as error bars. We refrained from error-prone and personally biased manual "cutting" of the track data for the sake of giving a more complete insight into skyrmion motion in a material with natural disorder. Especially problematic from the point of statistical variations is the skyrmion Hall angle. On the one hand, the impurities and grains in the material can lead to some deviation. Furthermore we observed thermal Brownian skyrmion motion, which can strongly affect the direction of motion[11,12] and distorts the velocity and the skyrmion Hall angle measurements, especially

in the low velocity regime. We gain a standard deviation of around 25° reaching up to 30° for individual measurements. To keep the plots readable, no error bars for θ_{Sk} are given, but the deviation of its value is given in the caption and the text.

C. Skyrmion motion in irradiated wires

Up to now, we have shown that we can stabilize skyrmions in the presented thin films, move them with current pulses in magnetic wires as depicted in Fig. 1 and statistically evaluate their motion. Now we want to figure out how we can tailor the motion of skyrmions using FIB irradiation. Here we present the results for two wires that are 25 μm and 35 μm wide. For a direct comparison, one half of the wire was kept pristine while the other half was irradiated, as indicated in Fig. 1, with 1.12×10^{12} ions/cm^2 and 2.3×10^{12} ions/cm^2. In the measurements it is evident that at the same current density, the skyrmion velocity in the irradiated part is largely reduced. In the plot in Fig. 4, velocity data for two wires treated with a different ion dose, is shown. For all measurements the main parameters ($\mu_0 H_{ext}$ =1.6 mT, t_{rise} =1.8 ns, t_{pulse} =50 ns, pulse number = 4) were fixed. The velocities in the pristine part are in good agreement for both wires. In the irradiated part, the current density needed to achieve reliable motion is stalled towards higher values. At the same time, the trend in the skyrmion Hall angle is remarkable. The angle is high and fluctuating for low current densities ($< 1.2 \times 10^{11}$ Am^{-2}), due to Brownian skyrmion motion. This thermally activated motion is also the reason for the non-zero velocity in that part of the plot that stays largely stable at around 1 m s^{-1}. This value however can not be considered to be the real thermally induced velocity as for the thermal motion not the 200 ns long current pulse (that is used to determine v_{Sk}) is relevant, but

the (unknown) timespan of the thermal motion. An upper bound for this time can be given by the exposure time of the camera (1 s). Using this value would result in a near-zero velocity for the Brownian motion case. As the exact time of the motion is unknown, we decided to use the same parameters as for the rest of the plot, knowingly overestimating the thermal skyrmion velocity.

In the medium current density range (1.2×10^{11} Am^{-2} to 1.7×10^{11} Am^{-2}), skyrmions in the pristine parts of the wire start to move with increasing velocity (see plot in Fig. 4 and (Multimedia view)). At the same time, the skyrmion Hall angle constantly stays at its lowest value around 20° as proposed for creep motion.[30] In the ion-treated part, the velocity stays at its initial low value of the Brownian motion. The angle of motion, however, steadily decreases to that of the pristine part.

In the higher end of the medium regime the skyrmions in both irradiated parts start to increase in velocity at around 1.5×10^{11} Am^{-2} and 1.55×10^{11} Am^{-2} for the lighter and the stronger irradiated part respectively. Also, an increasing electrical resistivity (lower current density) due to irradiation could explain this behaviour. However, we do not expect an increase in resistivity as high as 50 %, that would correspond to the measured results.

Moreover (DC) resistance measurements did not show a significant change of the resistance of the wire after irradiation. Furthermore we also investigated skyrmion motion in fully irradiated stripes and completely pristine wires. In the fully irradiated wire, also the skyrmion motion regime is shifted to higher current densities. This measurement excludes the effects of FIB-induced degradation of the electrical conductivity. For the high current density regime beyond 1.7×10^{11} Am^{-2} the velocity increases parallel for all four regions that we investigated. While θ_{Sk} remains low for the irradiated parts resembling the behavior of the pristine wire at lower current
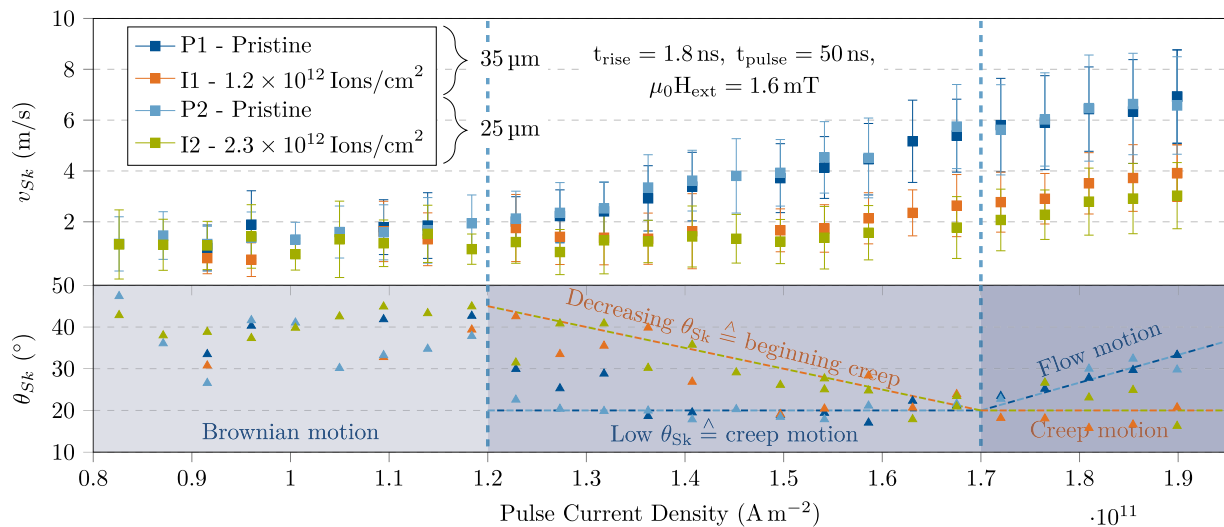

FIG. 4. Plot of the mean skyrmion velocity v_{Sk} in the upper part and the corresponding mean skyrmion Hall angles θ_{Sk} in the lower part. Data is presented for two magnetic wires with a pristine and an irradiated part each. Wire 1 consists of the parts P1 (blue) and I1 (orange) and combined is 35 μm wide with the parts being 17.5 μm wide, wire 2 (P2 and I2, light blue and green) is 25 μm wide and the parts are 12.5 μm each. All measurements were performed with t_{rise} =1.8 ns, t_{pulse} =50 ns and $\mu_0 H_{ext}$ =1.6 mT as denoted in the plot. Vertical lines separate Brownian motion, creep motion, and flow motion regime for the pristine (P) parts. Dashed lines are a guide to the eye clarifying the development of θ_{Sk}. While the standard deviation of θ_{Sk} is as high as ≈25°, and for sake of clarity not depicted, still a clear trend is visible. Videos of the skyrmion motion with varying current density are given in the (Multimedia view). Multimedia view: https://doi.org/10.1063/9.0000287.2

densities, the increase of θ_{Sk} for the pristine parts speaks for a transition to a flow motion regime. In the flow regime, the current is strong enough to depin the skyrmions. This results in a free motion and a skyrmion Hall angle that evolves towards its intrinsic value.

IV. CONCLUSION

Concluding we have shown that FIB can be used to alter velocity and the skyrmion Hall angle of current-driven skyrmions locally. Nonetheless, it still is of interest to understand in more detail the effects of annealing and irradiation on the magnetic properties of the thin film. Also, the proposed Néel-Brown model for the motion of skyrmions with different pulse-width still needs to be verified. From our point of view, also repeating the experiments with other skyrmion hosting material systems, especially those without Brownian motion, could be interesting and give more profound insight. Beyond physical properties, the irradiation technique's application for the realization of logic devices is of great interest. Even more, as focused ion beam technique is similar to a large extent to ion implantation used in nowadays semiconductor industry, and therefore can be considered industry-ready. Finally, we did not dig deeper into the possibilities of tuning the Brownian motion with FIB, e.g., for probabilistic computing devices.

SUPPLEMENTARY MATERIAL

See supplementary material for details on the current pulse measurements and the current density calculations.

ACKNOWLEDGMENTS

AUTHOR DECLARATIONS

Conflict of Interest

The authors have no conflicts to disclose.

DATA AVAILABILITY

The data that support the findings of this study are available from the corresponding author upon reasonable request.

REFERENCES

[1]S. Mühlbauer, B. Binz, F. Jonietz, C. Pfleiderer, A. Rosch, A. Neubauer, R. Georgii, and P. Böni, "Skyrmion lattice in a chiral magnet," Science **323**, 915–919 (2009).

[2]T. H. R. Skyrme, "A non-linear theory of strong interactions," Proceedings of the Royal Society of London. Series A. Mathematical and Physical Sciences **247**, 260–278 (1958).

[3]J. Müller, "Magnetic skyrmions on a two-lane racetrack," New Journal of Physics **19**, 025002 (2017).

[4]A. Fert, V. Cros, and J. Sampaio, "Skyrmions on the track," Nature Nanotechnology **8**, 152–156 (2013).

[5]R. Tomasello, E. Martinez, R. Zivieri, L. Torres, M. Carpentieri, and G. Finocchio, "A strategy for the design of skyrmion racetrack memories," Scientific Reports **4**, 6784–6787 (2014).

[6]F. Garcia-Sanchez, J. Sampaio, N. Reyren, V. Cros, and J.-V. Kim, "A skyrmion-based spin-torque nano-oscillator," New Journal of Physics **18**, 075011 (2016).

[7]M. Chauwin, X. Hu, F. Garcia-Sanchez, N. Betrabet, A. Paler, C. Moutafis, and J. S. Friedman, "Skyrmion logic system for large-scale reversible computation," Physical Review Applied **12**, 064053 (2019).

[8]S. Luo, M. Song, X. Li, Y. Zhang, J. Hong, X. Yang, X. Zou, N. Xu, and L. You, "Reconfigurable skyrmion logic gates," Nano Letters **18**, 1180–1184 (2018).

[9]L. Gnoli, F. Riente, M. Vacca, M. Ruo Roch, and M. Graziano, "Skyrmion logic-in-memory architecture for maximum/minimum search," Electronics **10**, 155 (2021).

[10]W. Kang, C. Zheng, Y. Huang, X. Zhang, Y. Zhou, W. Lv, and W. Zhao, "Complementary skyrmion racetrack memory with voltage manipulation," IEEE Electron Device Letters **37**, 924–927 (2016).

[11]T. Nozaki, Y. Jibiki, M. Goto, E. Tamura, T. Nozaki, H. Kubota, A. Fukushima, S. Yuasa, and Y. Suzuki, "Brownian motion of skyrmion bubbles and its control by voltage applications," Applied Physics Letters **114**, 012402 (2019).

[12]J. Zázvorka, F. Jakobs, D. Heinze, N. Keil, S. Kromin, S. Jaiswal, K. Litzius, G. Jakob, P. Virnau, D. Pinna et al., "Thermal skyrmion diffusion used in a reshuffler device," Nature Nanotechnology **14**, 658–661 (2019).

[13]W. Jiang, X. Zhang, G. Yu, W. Zhang, X. Wang, M. Benjamin Jungfleisch, J. E. Pearson, X. Cheng, O. Heinonen, K. L. Wang et al., "Direct observation of the skyrmion Hall effect," Nature Physics **13**, 162–169 (2017).

[14]R. Juge, K. Bairagi, K. G. Rana, J. Vogel, M. Sall, D. Mailly, V. T. Pham, Q. Zhang, N. Sisodia, M. Foerster et al., "Helium ions put magnetic skyrmions on the track," Nano Letters **21**, 2989–2996 (2021).

[15]S. Jaiswal, K. Litzius, I. Lemesh, F. Büttner, S. Finizio, J. Raabe, M. Weigand, K. Lee, J. Langer, B. Ocker et al., "Investigation of the Dzyaloshinskii-Moriya interaction and room temperature skyrmions in W/CoFeB/MgO thin films and microwires," Applied Physics Letters **111**, 022409 (2017).

[16]K. Zeissler, S. Finizio, C. Barton, A. J. Huxtable, J. Massey, J. Raabe, A. V. Sadovnikov, S. A. Nikitov, R. Brearton, T. Hesjedal et al., "Diameter-independent skyrmion Hall angle observed in chiral magnetic multilayers," Nature Communications **11**, 428 (2020).

[17]Y. Liu, N. Lei, C. Wang, X. Zhang, W. Kang, D. Zhu, Y. Zhou, X. Liu, Y. Zhang, and W. Zhao, "Voltage-driven high-speed skyrmion motion in a skyrmion-shift device," Physical Review Applied **11**, 014004 (2019).

[18]J. Feilhauer, S. Saha, J. Tobik, M. Zelent, L. J. Heyderman, and M. Mruczkiewicz, "Controlled motion of skyrmions in a magnetic antidot lattice," Physical Review B **102**, 184425 (2020).

[19]K. Fallon, S. Hughes, K. Zeissler, W. Legrand, F. Ajejas, D. Maccariello, S. McFadzean, W. Smith, D. McGrouther, S. Collin et al., "Controlled individual skyrmion nucleation at artificial defects formed by ion irradiation," Small **16**, 1907450 (2020).

[20]S. Zhang, A. K. Petford-Long, and C. Phatak, "Creation of artificial skyrmions and antiskyrmions by anisotropy engineering," Scientific Reports **6**, 31248 (2016).

[21]F. C. Ummelen, T. Lichtenberg, H. J. M. Swagten, and B. Koopmans, "Controlling skyrmion bubble confinement by dipolar interactions," Applied Physics Letters **115**, 102402 (2019).

[22]K. Garello, F. Yasin, H. Hody, S. Couet, L. Souriau, S. H. Sharifi, J. Swerts, R. Carpenter, S. Rao, W. Kim et al., "Manufacturable 300mm platform solution for field-free switching SOT-MRAM," in 2019 Symposium on VLSI Circuits (IEEE, 2019), pp. T194–T195.

[23]J.-Y. Tinevez, N. Perry, J. Schindelin, G. M. Hoopes, G. D. Reynolds, E. Laplantine, S. Y. Bednarek, S. L. Shorte, and K. W. Eliceiri, "TrackMate: An open and extensible platform for single-particle tracking," Methods **115**, 80–90 (2017).

[24]J. Schindelin, I. Arganda-Carreras, E. Frise, V. Kaynig, M. Longair, T. Pietzsch, S. Preibisch, C. Rueden, S. Saalfeld, B. Schmid et al., "Fiji: An open-source platform for biological-image analysis," Nature Methods **9**, 676–682 (2012).

[25]Y.-W. Oh, K.-D. Lee, J.-R. Jeong, and B.-G. Park, "Interfacial perpendicular magnetic anisotropy in CoFeB/MgO structure with various underlayers," Journal of Applied Physics **115**, 17C724 (2014).

[26] G.-G. An, J.-B. Lee, S.-M. Yang, J.-H. Kim, W.-S. Chung, and J.-P. Hong, "Highly stable perpendicular magnetic anisotropies of CoFeB/MgO frames employing W buffer and capping layers," Acta Materialia **87**, 259–265 (2015).

[27] D. M. Lattery, D. Zhang, J. Zhu, X. Hang, J.-P. Wang, and X. Wang, "Low gilbert damping constant in perpendicularly magnetized W/CoFeB/MgO films with high thermal stability," Scientific Reports **8**, 13395 (2018).

[28] S. Zhang, J. Zhang, Q. Zhang, C. Barton, V. Neu, Y. Zhao, Z. Hou, Y. Wen, C. Gong, O. Kazakova et al., "Direct writing of room temperature and zero field skyrmion lattices by a scanning local magnetic field," Applied Physics Letters **112**, 132405 (2018).

[29] G. Yu, P. Upadhyaya, Q. Shao, H. Wu, G. Yin, X. Li, C. He, W. Jiang, X. Han, P. K. Amiri et al., "Room-temperature skyrmion shift device for memory application," Nano Letters **17**, 261–268 (2017).

[30] C. Reichhardt and C. J. O. Reichhardt, "Thermal creep and the skyrmion Hall angle in driven skyrmion crystals," Journal of Physics: Condensed Matter **31**, 07LT01 (2018).

[31] W. F. Brown, Jr., "Thermal fluctuations of a single-domain particle," Physical Review **130**, 1677 (1963).

[32] W. Wernsdorfer, E. B. Orozco, K. Hasselbach, A. Benoit, B. Barbara, N. Demoncy, A. Loiseau, H. Pascard, and D. Mailly, "Experimental evidence of the Néel-Brown model of magnetization reversal," Physical Review Letters **78**, 1791 (1997).

[33] S. Mendisch, F. Riente, V. Ahrens, L. Gnoli, M. Haider, M. Opel, M. Kiechle, M. Ruo Roch, and M. Becherer, "Controlling domain-wall nucleation in Ta/Co-Fe-B/MgO nanomagnets via local Ga^+ ion irradiation," Phys. Rev. Applied **16**, 014039 (2021).

[34] J. Müller and A. Rosch, "Capturing of a magnetic skyrmion with a hole," Physical Review B **91**, 054410 (2015).